**Wind and Structures**, *Vol. 31, No. 3 (2020) 269-285*
DOI: https://doi.org/10.12989/was.2020.31.3.269


# Comparative analysis of the wind characteristics of three landfall typhoons based on stationary and nonstationary wind models

Yong Quan[a], Guo Qiang Fu[b], Zi Feng Huang[c] and Ming Gu*

*State Key Laboratory of Disaster Reduction in Civil Engineering, Tongji University, Shanghai 200092, China*

(*Received July 4, 2020, Revised August 5, 2020, Accepted August 8, 2020*)

**Abstract.** The statistical characteristics of typhoon wind speed records tend to have a considerable time-varying trend; thus, the stationary wind model may not be appropriate to estimate the wind characteristics of typhoon events. Several nonstationary wind speed models have been proposed by pioneers to characterize wind characteristics more accurately, but comparative studies on the applicability of the different wind models are still lacking. In this study, three landfall typhoons, Ampil, Jongdari, and Rumbia, recorded by ultrasonic anemometers atop the Shanghai World Financial Center (SWFC), are used for the comparative analysis of stationary and nonstationary wind characteristics. The time-varying mean is extracted with the discrete wavelet transform (DWT) method, and the time-varying standard deviation is calculated by the autoregressive moving average generalized autoregressive conditional heteroscedasticity (ARMA-GARCH) model. After extracting the time-varying trend, the longitudinal wind characteristics, e.g., the probability distribution, power spectral density (PSD), turbulence integral scale, turbulence intensity, gust factor, and peak factor, are comparatively analyzed based on the stationary wind speed model, time-varying mean wind speed model and time-varying standard deviation wind speed model. The comparative analysis of the different wind models emphasizes the significance of the nonstationary considerations in typhoon events. The time-varying standard deviation model can better identify the similarities among the different typhoons and appropriately describe the nonstationary wind characteristics of the typhoons.

**Keywords:** Field measurement; Landfall typhoons; Nonstationary wind characteristics; Time-varying mean; Time-varying standard deviation

## 1. Introduction

Typhoons, which are catastrophic natural disasters, cause enormous casualties and large economic losses to human society every year. The southeast coastal area of China is the most populous and prosperous region in China, with numerous super high-rise buildings and super long-span bridges, but the region is also one of the most severely affected regions by typhoons in the world (Xiao *et al*. 2011). In particular, from July to August 2018, three typhoons (Ampil, Jongdari, and Rumbia) successively made landfall in Shanghai, which makes Shanghai the first city in China to suffer three typhoon landfalls within 30 days in the Chinese meteorological recorded history. For super high-rise buildings, super long-span bridges, and other wind-sensitive structures, the wind-resistant design is the key factor in their structural design. Hence, the wind load and dynamic characteristics of structures under typhoon conditions have attracted widespread attention from scholars. Although the wind effects on wind-sensitive structures can be assessed via wind tunnel tests or numerical simulations, the typhoon wind field greatly differs from the synoptic wind field, and the accuracy of the above two methods highly depends on the precise modeling of the approaching wind fields (He *et al*. 2018). Therefore, field measurement, i.e., the direct observation of prototype structures, is still regarded as the most reliable and convincing approach and is also an important and long-term research field in wind engineering.

Over the past several decades, scholars have carried out extensive field measurements of typhoon wind characteristics on super high-rise buildings and long-span bridges, and fruitful results have been achieved (Chen and Xu 2004, Fu *et al.* 2012, Huang *et al.* 2019, Law *et al.* 2006, Li *et al*. 2015, Li and Hu 2015, Li *et al*. 2000, Li *et al*. 2007, Li *et al*. 2003, Pan *et al*. 2017, Song *et al*. 2012, Wang *et al*. 2013, Wang *et al*. 2017, Wu *et al*. 2019, Xu *et al*. 2017, Zhi *et al*. 2011). However, it should be pointed out that most of the field measurements above are based on the assumption that the wind speed is a stationary ergodic random process, which neglects the inherent time-varying characteristics of the statistics of wind speed records. Recent field measurements indicate that the wind speed samples collected during typhoon events exhibit strong nonstationary features (Chen and Xu 2004, Wang *et al*. 2016a, Xu *et al*. 2000), that is, there are considerable time-dependent variations in the mean value, variance, or their combination (McCullough and Kareem 2013).

*Corresponding author, Professor
E-mail: minggu@tongji.edu.cn
[a]Professor
E-mail: quanyong@tongji.edu.cn
[b]Ph.D. Candidate
E-mail: fuguoqiang@tongji.edu.cn
[c]Ph.D.
E-mail: zifengh22@163.com



ISSN: 1226-6116 (Print), 1598-6225 (Online)

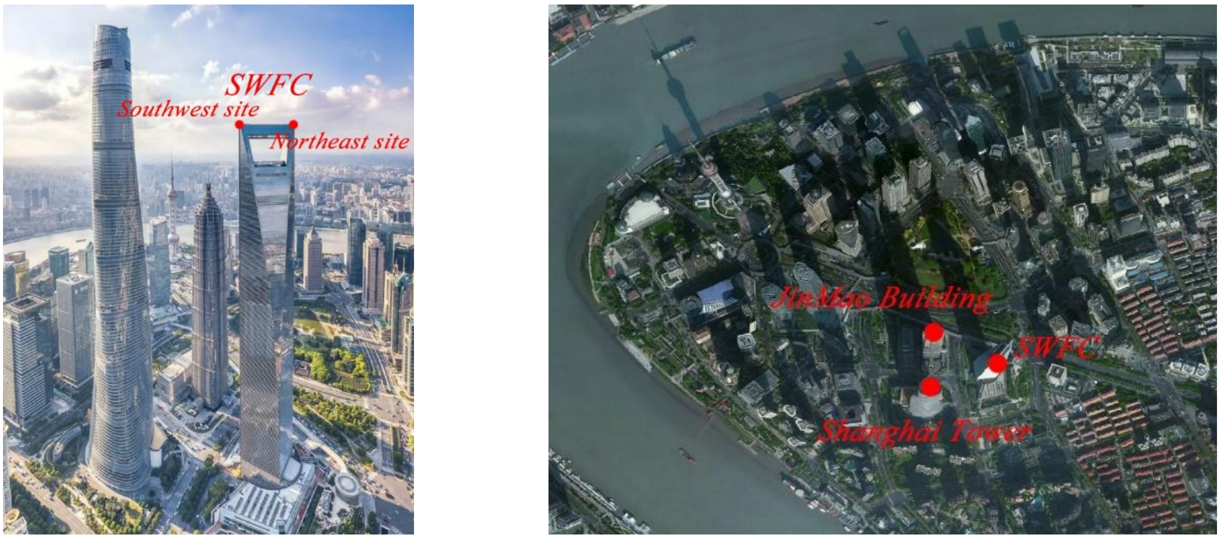


(a) Aerial view (b) Satellite Image

Fig. 1 Location of the Shanghai World Financial Center and surroundings

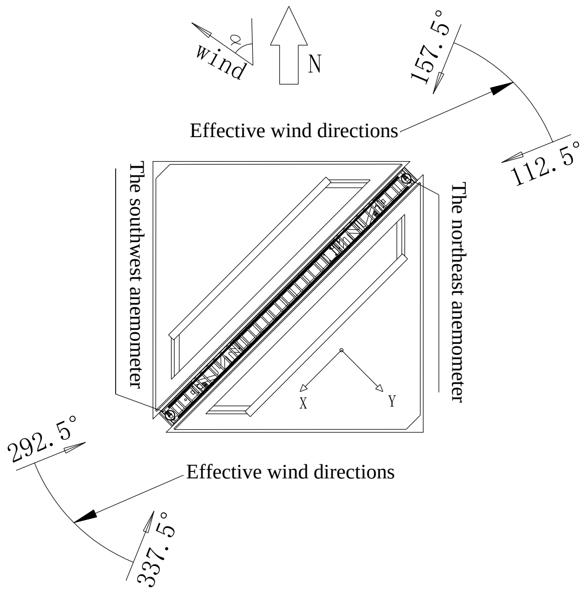


Fig. 2 Sketch of the location and effective directions of the ultrasonic anemometers

To understand the wind characteristics of typhoons and their effects on structures more precisely, several nonstationary wind speed models have been proposed by pioneers (Chen and Letchford 2005, Xu and Chen 2004), which can be classified into two categories, the time-varying mean wind speed model and the time-varying standard deviation wind speed model. The time-varying mean wind speed model only considers the time-varying mean wind speed, while the non-stationarity of both the time-varying mean and the time-varying standard deviation of the wind speed are taken into account in the time-varying standard deviation wind speed model.

Based on nonstationary wind speed models, pioneering works on the comparative studies of stationary and nonstationary wind characteristics have been conducted. Chen *et al*. (2006) investigated the difference in wind characteristics obtained by the stationary and time-varying mean wind speed models using wind speed data from both monsoons and typhoons. Tao *et al*. (2016b) proposed awavelet-based self-adaptive approach to extract the time-varying mean according to the signal stationarity, and the wind characteristics of Typhoon Fung-Wong were comparatively analyzed in detail. In addition, He *et al.* (2017), Tao *et al.* (2016a), Wang *et al.* (2016b), and Yu *et al.* (2019) conducted comparative studies of stationary and nonstationary wind characteristics using field-measured wind speed data. Nevertheless, these comparative studies mainly focus on the time-varying trend of the mean wind speed in wind records, thereby ignoring the time-varying trend of the standard deviation in the fluctuating wind speed. There are still insufficient comparative studies on the discrepancies between the time-varying mean wind speed model and the time-varying standard deviation wind speed model. To increase the awareness of the applicability of the

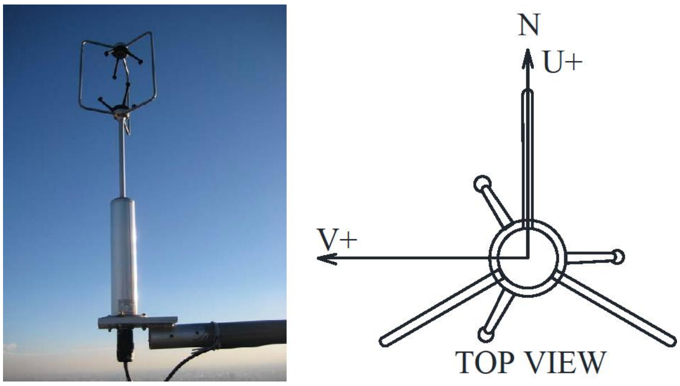


Fig. 3 Windmaster Pro ultrasonic anemometer and definition of its U- and V-axes

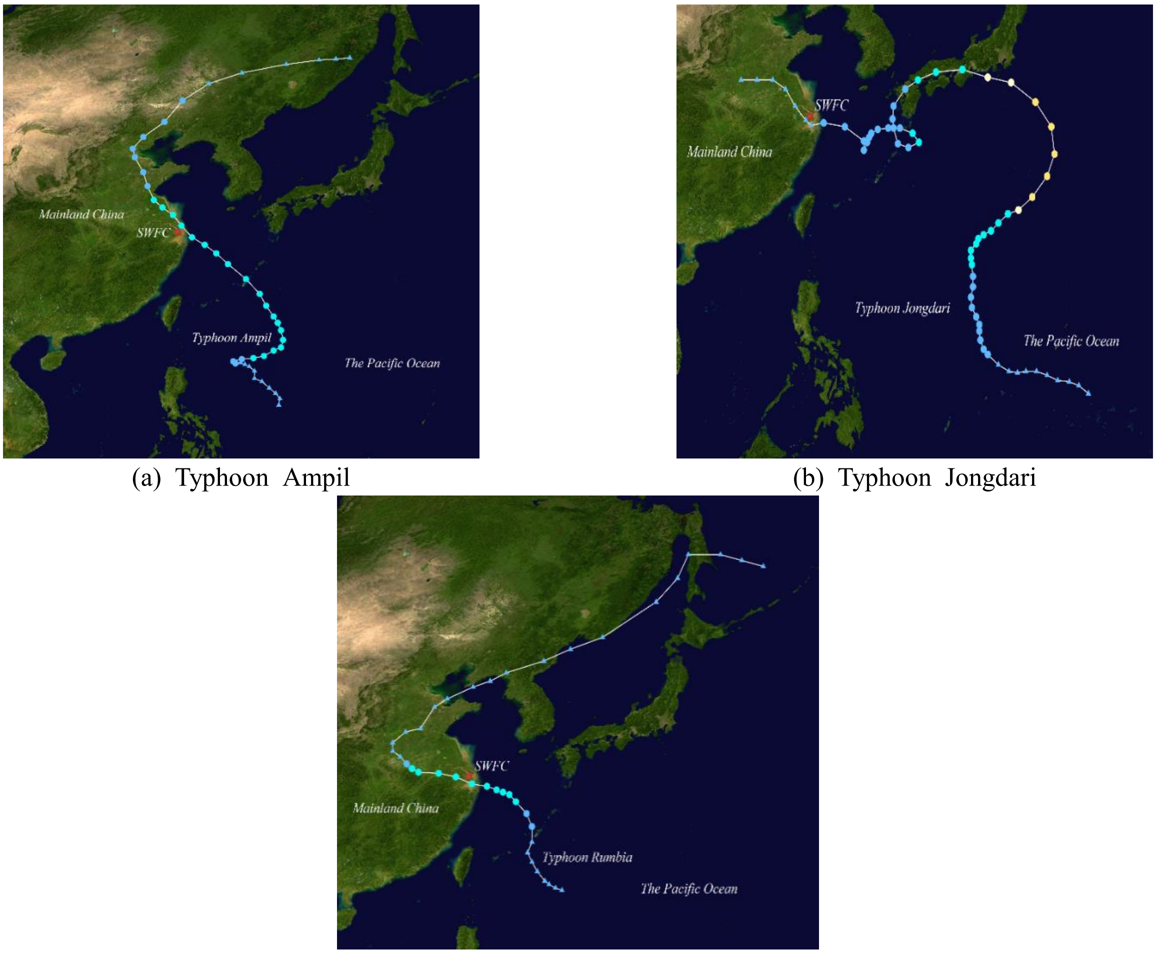


(a) Typhoon Ampil

(b) Typhoon Jongdari

(c) Typhoon Rumbia

Fig. 4 Paths of the three typhoons

different wind speed models in analyzing the wind characteristics of typhoons, it is of great significance to perform detailed comparative analysis studies.

In this article, three landfall typhoons, namely, Ampil, Jongdari, and Rumbia, recorded by the ultrasonic anemometers atop the Shanghai World Financial Center (SWFC), are selected for the comparative analysis of wind characteristics. The discrete wavelet transform (DWT) method is adopted to extract the time-varying mean wind speed, and the time-varying standard deviation is calculated by the autoregressive moving average generalized autoregressive conditional heteroscedasticity (ARMA-GARCH) model (Huang and Gu 2019a). Then, the longitudinal wind characteristics of the three typhoons, including the probability distribution, power spectral density (PSD), turbulence integral length scale, turbulence intensity, gust factor, and peak factor, are comparatively analyzed based on the stationary model, time-varying mean model, and time-varying standard deviation model. Several results are derived, and conclusions are drawn in the end. It is anticipated that the data and analysis results in this paper could provide references for the structural wind-resistant

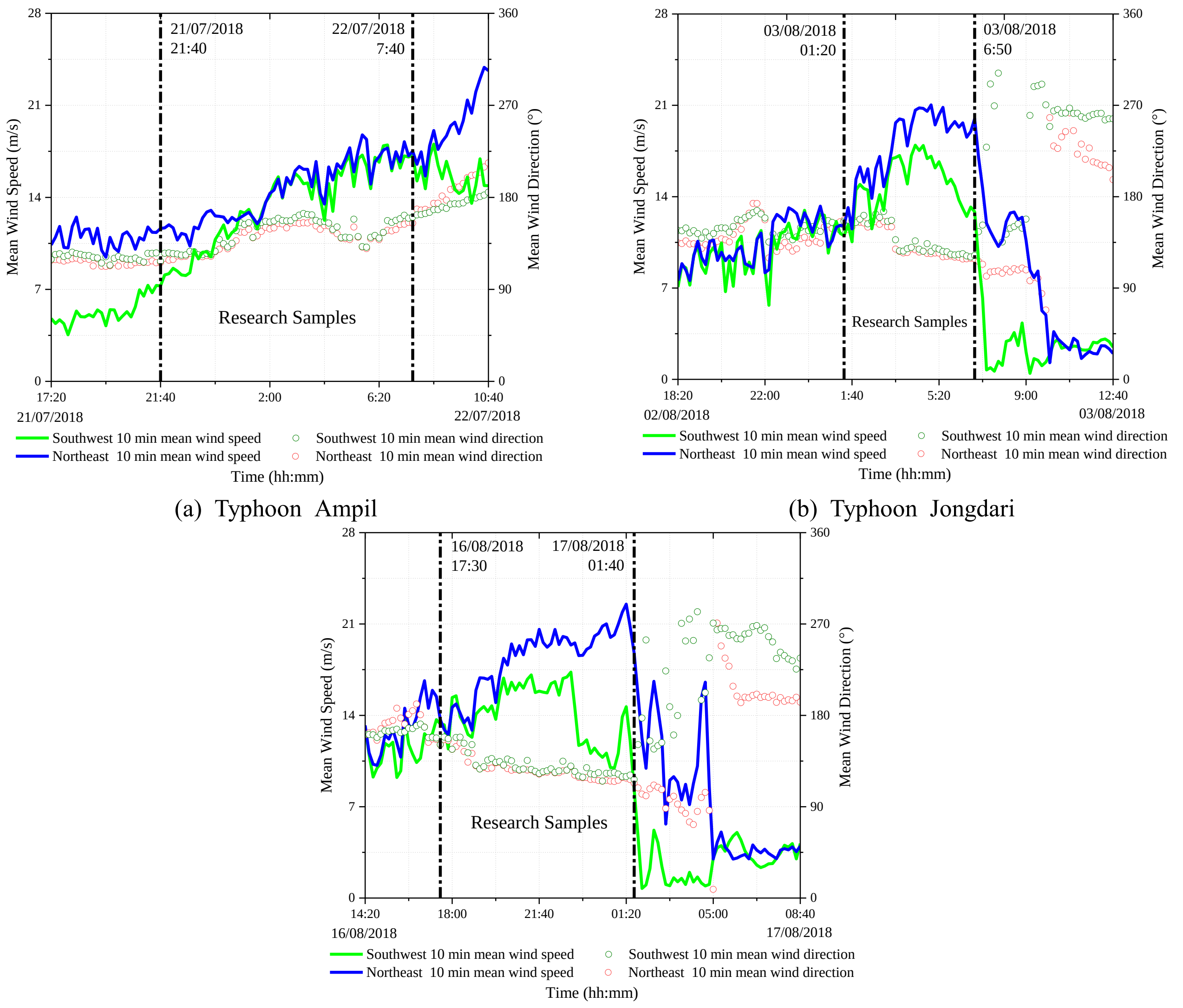


(a) Typhoon Ampil (b) Typhoon Jongdari

(c) Typhoon Rumbia

Fig. 5 Comparison of the 10 min mean wind speeds and mean wind directions from the northeast and southwest anemometers during the three typhoons

design of super high-rise buildings and enrich the nonstationary typhoon wind characteristics database.

## 2. Overview of the field measurements and typhoons

### *2.1 Introduction of the field measurements*

The SWFC, located in the Lujiazui financial district, mainland China, is a super high-rise building with a height of 492 m above the ground and consists of 101 stories. The SWFC is also the sixth tallest building in mainland China and the eleventh tallest building in the world. The SWFC is surrounded by a large number of super high-rise buildings, such as the Jin Mao Building (421 m) and the Shanghai Tower (632 m), which are located approximately 170 m to the northwest and 210 m to the southwest of the SWFC, respectively. The wind environment around the SWFC belongs to the typical rough urban underlying surface environment, which makes the near-ground wind characteristics extremely complex. Fig. 1 shows the location of the SWFC and surrounding buildings.

Two Windmaster Pro ultrasonic anemometers (Gill Instruments, U.K.) are installed at the northeast and southwest corners atop the SWFC (497 m), as shown in Fig. 2. The horizontal distance between the two instruments is 71.6 m. As shown in Fig. 3, the U-, V-, and W-axes of the anemometers face north, west, and upward directions, respectively. The wind direction increases along the counter clockwise direction as viewed from the top. For instance, the 0-degree wind direction marks the southerly wind, and the easterly wind is 90-degree wind direction. The measurement range of the ultrasonic anemometer spans from 0.01 to 65 m/s, with the actual sampling frequency of 10 Hz. Real-time storage of the acquired data is achieved by a CR1000 data collection system (Campbell Co. Ltd., U.S.A.). According to computational fluid dynamics simulations of the wind field surrounding the SFWC, the mean and fluctuating wind speeds approaching the target building are influenced by the building itself, the parapet

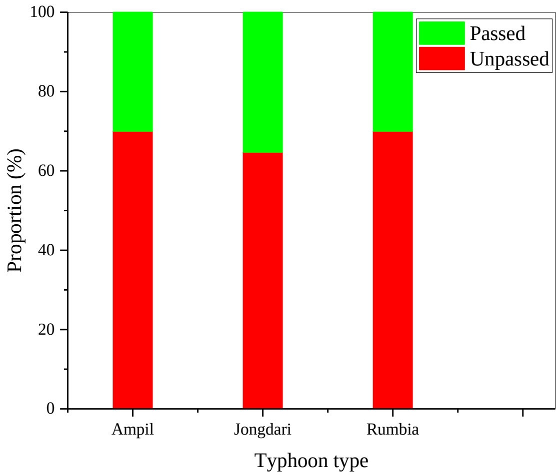


(a) Mean value

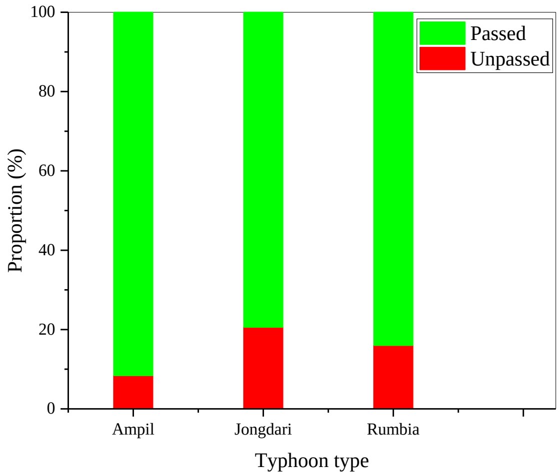


(b) Standard deviation

Fig. 6 Stationary evaluation of the wind speed samples of the three typhoons in terms of the mean value or standard deviation

walls, and the window-cleaning machines. However, these influences are negligible when the included wind direction between the approaching wind and the x-axis of the building is smaller than 22.5°. Thus, the effective wind direction range of the northeast site is 112.5-157.5° and that of the southwest site is 292.5-337.5° (An et al. 2012, Quan et al. 2013, Huang and Gu 2019a) as shown in Fig. 2.

### *2.2 Description of the three typhoons*

From July to August 2018, Typhoons Ampil, Jongdari, and Rumbia successively made landfall in Shanghai. The ultrasonic anemometers atop the SWFC successfully collected wind speed and wind direction data of the three typhoons. Fig. 4 shows the paths of the three typhoons.

#### *2.2.1 Typhoon ampil*

Typhoon Ampil was the tenth tropical cyclone in 2018. The typhoon was born as a tropical storm on the surface of the northwestern Pacific Ocean and moved in a northwestward direction on July 18. On July 20, the tropical storm evolved into a severe tropical storm and continued to move northwest. The typhoon made landfall on the island of Chongming in Shanghai at 12:30 p.m. local time (UTC+8) on July 20, with winds of up to 28 meters per second near its eye. Then, the typhoon moved towards the west-northwest as its intensity began to decrease. On July 24, Typhoon Ampil weakened to an extratropical cyclone and finally disappeared the next day. During its landfall in Shanghai, the nearest distance between the SWFC and the path of Ampil is 48 km.

#### *2.2.2 Typhoon Jongdari*

Typhoon Jongdari was a strong, long-lived and anomalous tropical cyclone that severely impacted Japan and China. Born as the twelfth tropical cyclone near Okinotorishima on July 24, 2018, it gradually intensified and moved towards southern Japan. Affected by an upper-level low and a subtropical ridge, Jongdari executed a rare counterclockwise route. The typhoon made landfall in the Kii Peninsula over the Mie Prefecture of Japan on July 29. Then, Jongdari gradually weakened as it moved along an anomalous route from east to west. On July 30, Jongdari entered the East China Sea with its intensity remaining in the tropical storm category. On August 3, the typhoon made landfall again in the coastal Jinshan District in southwest Shanghai at 10:30 a.m. local time (UTC+8), with winds of up to 23 meters per second near its eye. Then, the typhoon headed towards the northwest with its intensity gradually decreasing. During its passage through Shanghai, the nearest distance between the SWFC and the path of Jongdari is 47 km.

#### *2.2.3 Typhoon Rumbia*

Typhoon Rumbia was the eighteenth tropical cyclone in 2018, and the third typhoon that made direct landfall in Shanghai within 30 days. On August 15, a tropical depression in the East China Sea developed into a tropical storm named Rumbia. It moved towards the northwest and gradually intensified. Rumbia evolved into a severe tropical storm on August 16. The typhoon made landfall at approximately 4:00 a.m. local time (UTC+8) on July 20 in the Pudong New Area, Shanghai, along with torrential rains and strong winds of up to 23 meters per second near its eye. Afterward, the typhoon moved towards the northwest with its intensity gradually decreasing. Rumbia became an extratropical cyclone over the northern Yellow Sea and disappeared on August 21. During its landfall in Shanghai, the nearest distance between the SWFC and the path of Rumbia is 18 km.

### *2.3 Data source of the three typhoons*

With the vector decomposition method, the wind speed records of the three typhoons are decomposed into longitudinal, lateral, and vertical wind speeds. In this study, the longitudinal wind speeds recorded by the northeast ultrasonic anemometers were selected for analysis. The averaging time interval $T$ for analysis of the wind characteristics is chosen as 10 min. To validate the quality of the field-measured data, the wind samples simultaneously collected by the southwest ultrasonic anemometer are used for comparison. The 10 min mean wind speeds and mean wind directions collected by the northeast and southwest ultrasonic anemometers during the three typhoons are presented for comparison in Fig. 5. The trends of the mean wind speed from the northeast and southwest are similar, and the mean wind directions coincide well with each other in the effective wind direction range, which indicates that the wind samples selected for analysis in this study are reliable.

To exclude the influences of the building itself, the parapet walls, and the window-cleaning machines, consecutive wind speed data within the effective wind direction range and 10 min mean wind speeds higher than 10 m/s are selected as research data for analysis, as shown in Fig. 5. For Typhoon Ampil, 600 mins of consecutive wind speed data from 21:40 p.m. on July 21 to 07:40 a.m. on July 22 are selected for analysis. The total average wind speed is 14.55 m/s, and the maximum 10 min mean wind speed is 18.75 m/s. For Typhoon Jongdari, 340 min of consecutive wind speed data from 01:20 a.m. on August 3 to 06:50 a.m. on August 3 are selected for analysis. The total average wind speed is 15.42 m/s, and the maximum 10 min mean wind speed is 21.04 m/s. For Typhoon Rumbia, 500 min of consecutive wind speed data from 17:30 p.m. on August 16 to 01:40 a.m. on August 17 are selected for analysis. The total average wind speed is 17.53 m/s, and the maximum 10 min mean wind speed is 22.53 m/s.

Due to environmental variability, noise, or other effects, the original longitudinal wind speed samples may contain outliers, which would affect the statistical analysis of the extreme value of wind speed. Therefore, these outliers were removed before analysis of the wind characteristics to guarantee the quality of the field-measured wind speed data. The specific process entails that for each sampling datum ($dat(t_i)$) of the longitudinal wind speed sample, ten sampling datums in total (five sampling datums before and after $dat(t_i)$, i.e., $dat(t_{i-5})\dots dat(t_{i-1})$, $dat(t_{i+1})\dots dat(t_{i+5})$. The intervals of different sampling datums are 0.1 sec, corresponding to the sampling frequency 10 Hz), are used to calculate the mean $\bar{U}_{i\pm5}$ and standard deviation $\sigma_{i\pm5}$. If $dat(t_i) \notin \left[\bar{U}_{i\pm5} - \sigma_{i\pm5}, \bar{U}_{i\pm5} + \sigma_{i\pm5}\right]$, then $dat(t_i)$ is regarded as an outlier and replaced with the linearly interpolated value in terms of the two data points before and after $dat(t_i)$.

### 2.4 Stationarity evaluation

In this study, the stationarity of the longitudinal wind speed samples collected from the three typhoons is evaluated in advance by the run test method in terms of the mean value and standard deviation (Bendat and Piersol 2011). The desired level of significance is 5%. Fig. 6 depicts the proportion of the wind speed samples that passes the stationarity evaluation and that of the wind speed samples that does not pass.

As shown in Fig. 6, in terms of the mean value, the proportions of wind speed samples that do not pass are 70%, 64.7%, and 70% for Typhoons Ampil, Jongdari, and Rumbia, respectively. The proportions of wind speed samples that do not pass in terms of the standard deviation are 8.3%, 20.6%, and 16% for Typhoons Ampil, Jongdari, and Rumbia, respectively. In general, the mean values show a significant nonstationary trend for the three typhoons, while the non-stationarity of the variance is relatively weak, but both types of non-stationarity cannot be ignored.

## 3. Wind speed models and analysis methods

### 3.1 Wind speed models

In the traditional stationary wind model, the wind speed is considered as a stationary ergodic random process (Simiu and Scanlan 1996). Thus, the wind speed consists of a constant mean wind speed and a zero-mean stationary fluctuating wind speed, detail as Eq. (1)

$$U(t) = \bar{U} + u(t) \tag{1}$$

where $U(t)$ = the longitudinal wind speed; $\bar{U}$ = the constant mean wind speed over time interval $T$; and $u(t)$ = the zero-mean fluctuating wind speed. The aforementioned wind speed model is called the stationary model in this study.

To analyze the nonstationary characteristics of the wind speed, many scholars have proposed their own wind speed models (Xu and Chen 2004, Chen and Letchford 2005). In this study, the two nonstationary wind models proposed by Xu and Chen (2004) and Chen and Letchford (2005) are adopted to comparatively analyze nonstationary wind characteristics.

Xu and Chen (2004) proposed to treat the nonstationary wind speed as a deterministic time-varying mean wind speed plus a zero-mean stationary fluctuating wind speed, as presented in Eq. (2)

$$U(t) = U^*(t) + u^*(t) \tag{2}$$

where $U(t)$ = the longitudinal wind speed; $U^*(t)$ = the deterministic time-varying mean wind speed, reflecting the temporal trend of the wind speed, which is derived by the DWT method in this study; and $u^*(t)$ = the zero-mean fluctuating wind speed. This wind speed model, named the time-varying mean model in this study, only considers the time-varying trend of the mean wind speed while neglecting the time-varying trend of the standard deviation of the fluctuating wind speed.

Chen and Letchford (2005) noted that the longitudinal nonstationary wind speed can be modeled as a deterministic time-varying mean wind speed plus a zero-mean uniformly modulated nonstationary process. Thus, the longitudinal wind speed can be expressed as Eq. (3)

$$\begin{cases} U(t) = U^{\Delta}(t) + u^{\Delta}(t) \\ u^{\Delta}(t) = \sigma_u{}^{\Delta}(t)\alpha_u{}^{\Delta}(t) \end{cases} \tag{3}$$

where $U(t)$ = the longitudinal wind speed; $U^{\Delta}(t)$ = the deterministic time-varying mean wind speed, the same as the time-varying mean model; $\sigma_u{}^{\Delta}(t)$ = the deterministic time-varying standard deviation, which is calculated by the ARMA-GARCH model in this study; and $\alpha_u{}^{\Delta}(t)$ = the stationary normalized fluctuating component with unit standard deviation. The time-varying trend of both the mean wind speed and the standard deviation of the fluctuating wind speed are taken into account in this wind speed model. The model is hereinafter referred to as the time-varying STD model.

Clearly, the time-varying STD model is the most generalized wind speed model among the three wind speed models above. When the fluctuating wind speed is a stationary random process after extracting the time-varying average wind speed, the time-varying standard deviation will become a constant, and Eq. (3) will degenerate into the time-varying mean model. If the wind speed is a stationary random process, the mean wind speed will become a constant, and Eq. (2) will also degenerate into the stationary model. A comparative analysis of the differences between the three wind speed models above will be conducted in the following sections based on the collected wind speed samples of the three typhoons.

### 3.2 Extraction of the time-varying mean values

Extracting the time-varying mean wind speed is a critical step when utilizing nonstationary wind models to analyze wind characteristics (Su *et al.* 2015). The DWT method is an efficient and convenient method to analyze nonstationary signals. Based on a series of basic functions that are dilated and translated from a mother wavelet, the DWT method decomposes broadband signal $X(t)$ into a sequence of successive narrow-band components, i.e.,

$$X(t)=\sum_{i=1}^{N} D_i(t)+A_N(t) \tag{4}$$

where $N$ is the total number of decomposition levels, $D_i(t)$ is the detailed component at level *i*, and $A_n(t)$ is the approximation component. As the number of levels increases, the frequency of the approximation $A_n(t)$ becomes lower and thus could represent the time-varying mean of $X(t)$. The DWT method with Daubechies wavelet of order 10 is adopted to derive the time-varying mean in this study. For each sample of the longitudinal wind speed, to ensure that the frequency of the time-varying mean is lower than 0.0015 Hz (far away from the fundamental frequency of the SWFC), the decomposition level is selected that minimizes the zero-mean fluctuating component's absolute value of the test statistic, which is evaluated with the run test in terms of the mean value of the segment (Bendat and Piersol 2011), for decomposition in the DWT method. The component of the lowest frequency obtained after decomposition is taken as the time-varying mean of the wind speed sample.

### 3.3 Extraction of the time-varying standard deviation

Numerical simulations and field measurements conducted by scholars have shown that it is practical to model the nonstationary fluctuating wind speed as a uniformly modulated nonstationary process (Huang *et al.* 2013, Huang *et al.* 2015). A key issue in the analysis of a uniformly modulated nonstationary process is the derivation of the time-varying standard deviation. The ARMA-GARCH model is an efficient method for the analysis of uniformly modulated process (Huang and Gu 2019a). The method first analyzes the uniform modulation nonstationary random process $x(t)=\sigma_x(t)\alpha_x(t)$ with the ARMA model to obtain the residual. Then, the GARCH model is utilized to estimate the time-varying standard deviation of the residual, and the time-varying standard deviation of the target process can be calculated accordingly.

$$\begin{cases} \phi(B)x(t)=\theta(B)\varepsilon(t) \\ \phi(B)=1+a_1B+a_2B^2+\dots a_pB^p \\ \theta(B)=1+b_1B+b_2B^2+\dots b_qB^q \\ \varepsilon(t)=\sigma_\varepsilon(t)w(t) \\ \sigma_\varepsilon(t)^2=E\left[\varepsilon(t)^2\right]=\gamma+\sum_{i=1}^{m}v_i\sigma_\varepsilon(t-i)^2+\sum_{j=1}^{l}\lambda_j\varepsilon(t-j)^2 \end{cases} \tag{5}$$

where $\sigma_x(t)$ is the time-varying standard deviation of the target process $x(t)$; $\alpha_x(t)$ is the stationary normalized component; $a_1,a_2,\dots a_p$ are the AR parameters; $b_1,b_2,\dots b_q$ are the MA parameters; *p* and *q* are the orders of AR(*p*) and MA(*q*), respectively; *B* is the backshift operator; $\phi$ (*B*) is the AR(*p*) polynomial and $\theta(B)$ is the MA(*q*) polynomial; residual $\varepsilon(t)$ is a zero-mean heteroscedasticity series with time-varying standard deviation $\sigma_\varepsilon(t)$; $w(t)$ is the zero-mean independent identically distributed white noise with unit standard deviation; $\gamma$, $\eta_i$, and $\lambda_j$ are parameters of the GARCH model; and *m* and *l* are the orders of the GARCH model. The time-varying variance in $x(t)$ can be calculated as follows

$$\sigma_x(t)^2=\mathrm{E}\left[x^2(t)\right]=\sigma_\varepsilon^2(t)\cdot\frac{\sum_{t=1}^{z}x^2(t)}{\sum_{t=1}^{z}\varepsilon^2(t)} \tag{6}$$

where *z* is the size of $x(t)$. The PSD $S_\alpha(f)$ of $\alpha_x(t)$ can be obtained from the following equation

$$S_\alpha(f)=\frac{\sigma_\varepsilon^2(t)}{\sigma_x^2(t)}\left|\frac{\theta\left(e^{i2\pi f}\right)}{\phi\left(e^{i2\pi f}\right)}\right|^2=\frac{\sum_{j=1}^{z}\varepsilon^2(t)}{\sum_{j=1}^{z}x^2(t)}\left|\frac{\theta\left(e^{i2\pi f}\right)}{\phi\left(e^{i2\pi f}\right)}\right|^2 \tag{7}$$

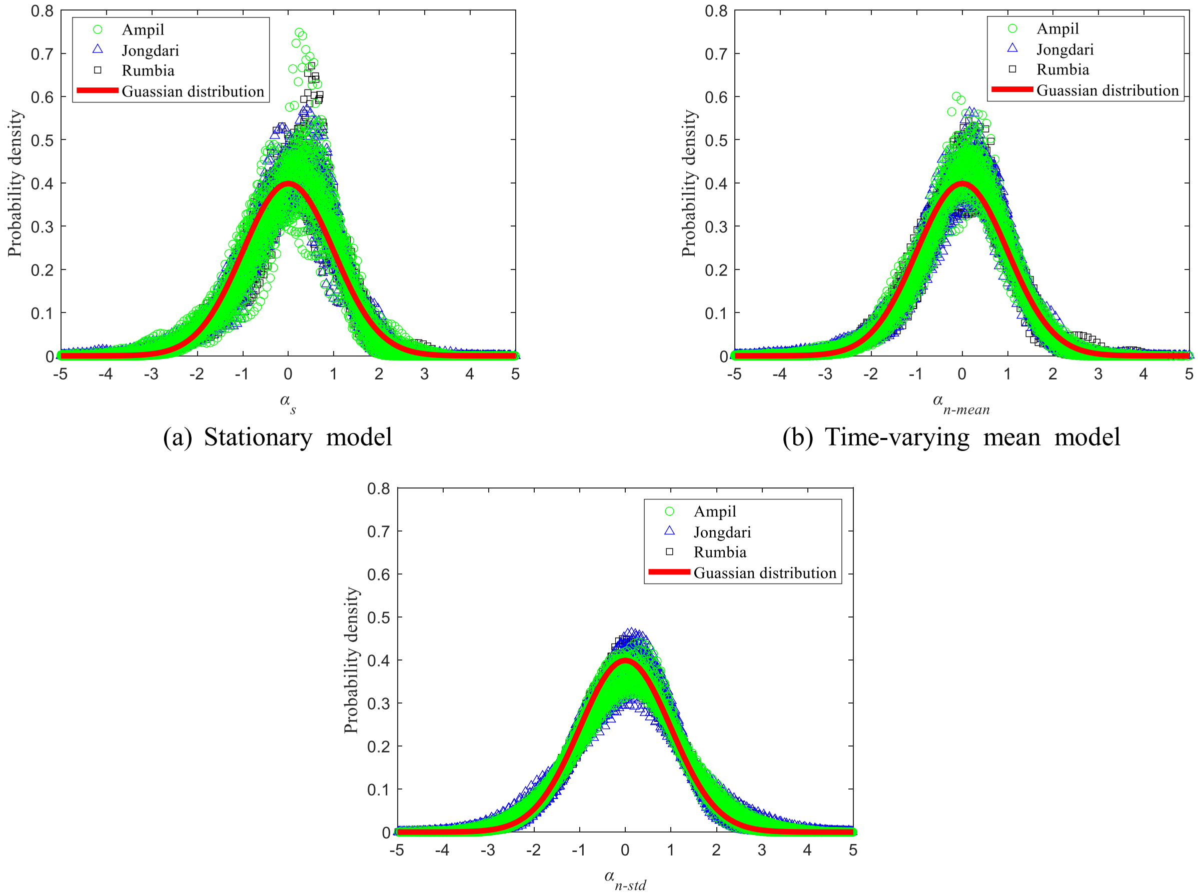


(a) Stationary model (b) Time-varying mean model

(c) Time-varying STD model

Fig. 7 Probability density distributions of the normalized fluctuating component based on the stationary model, time -varying mean model, and time-varying STD model for the three typhoons

where $f$ is the frequency (Hz). More details about the ARMA-GARCH model can be found in Huang and Gu (2019a). In the time-varying STD model, the ARMA-GARCH model is adopted to estimate the time-varying standard deviation of the fluctuating wind speed.

## 4. Analysis of the fluctuating wind characteristics

Based on the consecutive and effective research samples of the three typhoons recorded atop the SWFC, the longitudinal wind characteristics such as the probability distribution, PSD, turbulence integral scale, turbulence intensity, gust factor, and peak factor were comparatively analyzed in detail.

### 4.1 Probability density distribution

The probability distribution of the longitudinal wind speed is generally considered to follow the Gaussian distribution. However, recent field measurements have shown that the distribution may not follow the Gaussian distribution (Balderrama *et al.* 2012, Hui *et al.* 2017). To reasonably compare the differences among the three wind models, the normalized fluctuating components in the three wind speed models are used for comparisons. The normalized fluctuating components in the stationary model are obtained by firstly subtracting the mean wind speed from the original wind speed time history and then dividing the standard deviation of fluctuating wind speed. The normalized fluctuating components in the time-varying mean model are obtained by firstly subtracting the time-varying mean wind speed from the original wind speed time history and then dividing the standard deviation of fluctuating wind speed. The normalized fluctuating components in the time-varying STD model are obtained by firstly subtracting the time-varying mean wind speed from the original wind speed time history and then dividing the time-varying standard deviation of fluctuating wind speed. $\alpha_s$, $\alpha_{n\text{-}mean}$, and $\alpha_{n\text{-}std}$ represent the normalized fluctuating components referring to the stationary model, time-varying mean model, and time-varying STD model, respectively. Then the probability density functions (PDFs) of the normalized fluctuating components of the three wind models are selected for analysis, as shown in Fig. 7. The standard Gaussian distribution is also shown in the figures for comparison.

As illustrated in Fig. 7, for each wind speed model, the main body shapes of the PDFs of the three typhoons' longitudinal normalized fluctuating components are similar.

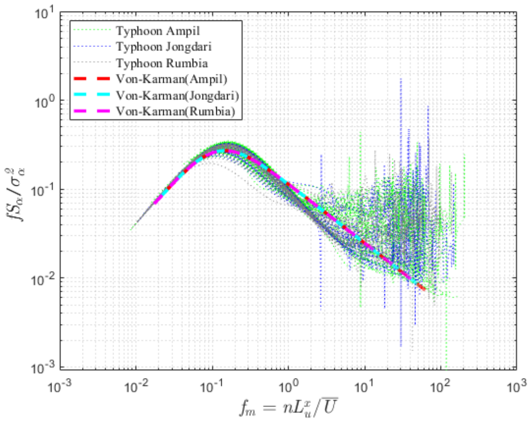


(a) Stationary model

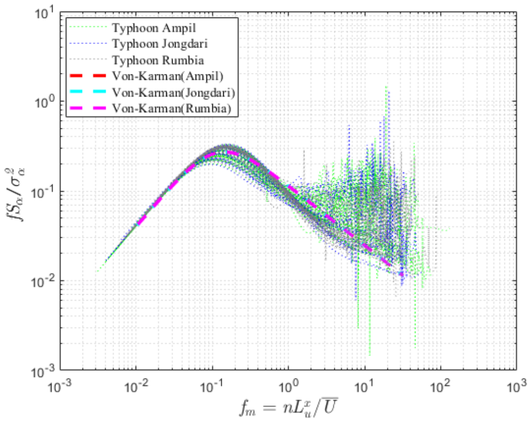


(b) Time-varying mean model

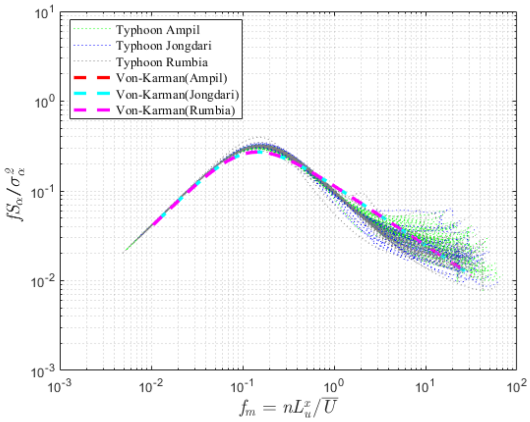


(c) Time-varying STD model

Fig. 8 Probability density distributions of the normalized fluctuating component based on the stationary model, time -varying mean model, and time-varying STD model for the three typhoons

Compared with the standard Gauss distribution, the PDFs of the three wind speed models show varying degrees of differences. The PDFs of the time-varying STD model are the closest to the standard Gaussian distribution, and the dispersion of the different typhoons is minimal. Despite the three typhoons having their own characteristics, the geomorphological characteristics around the observation site have not changed during the period, and therefore, the fluctuating wind speed should have certain common features. The above analysis indicates that the time-varying STD model can better capture the similarities of the longitudinal normalized fluctuating components.

### *4.2 Power spectral density and turbulence integral scale*

The PSD of the fluctuating wind speed describes the kinetic energy contributions of vortices of different sizes to the total turbulent kinetic energy. The turbulence integral scale defines several representative vortex scales with certain features to represent the average scale of the vortices in turbulence. In this study, the PSD $S_\alpha(f)$ of each longitudinal normalized fluctuating component $\alpha(t)$ is calculated with the orders and parameters of the ARMA model according to Eq.(7). The longitudinal turbulence integral scale $L_u^x$ is obtained by fitting the $S_\alpha(f)$ values in the form of a general wind spectrum, which is expressed as (Huang and Gu 2019a):

$$\begin{cases} \dfrac{fS_\alpha(f)}{\sigma_\alpha^2} = \dfrac{4f_m}{(1+Gf_m{}^b)^c} \\ f_m = \dfrac{fL_u^x}{\overline{U}} \end{cases} \tag{8}$$

where $\sigma_\alpha$ is the standard deviation of the normalized fluctuating component $\alpha(t)$; $f$ is the frequency (Hz); $G$, $b$, and $c$ are fitting parameters; and $\overline{U}$ is the mean wind speed.

Fig. 8 displays the PSDs of the longitudinal normalized fluctuating components $\alpha(t)$ of the three wind speed models. The measured spectra of the stationary model and the time-varying mean model are concentrated in the large-eddy region, with a certain degree of dispersion in the inertia subregion and the largest dispersions in the high-frequency region. It may result from the non-stationarities

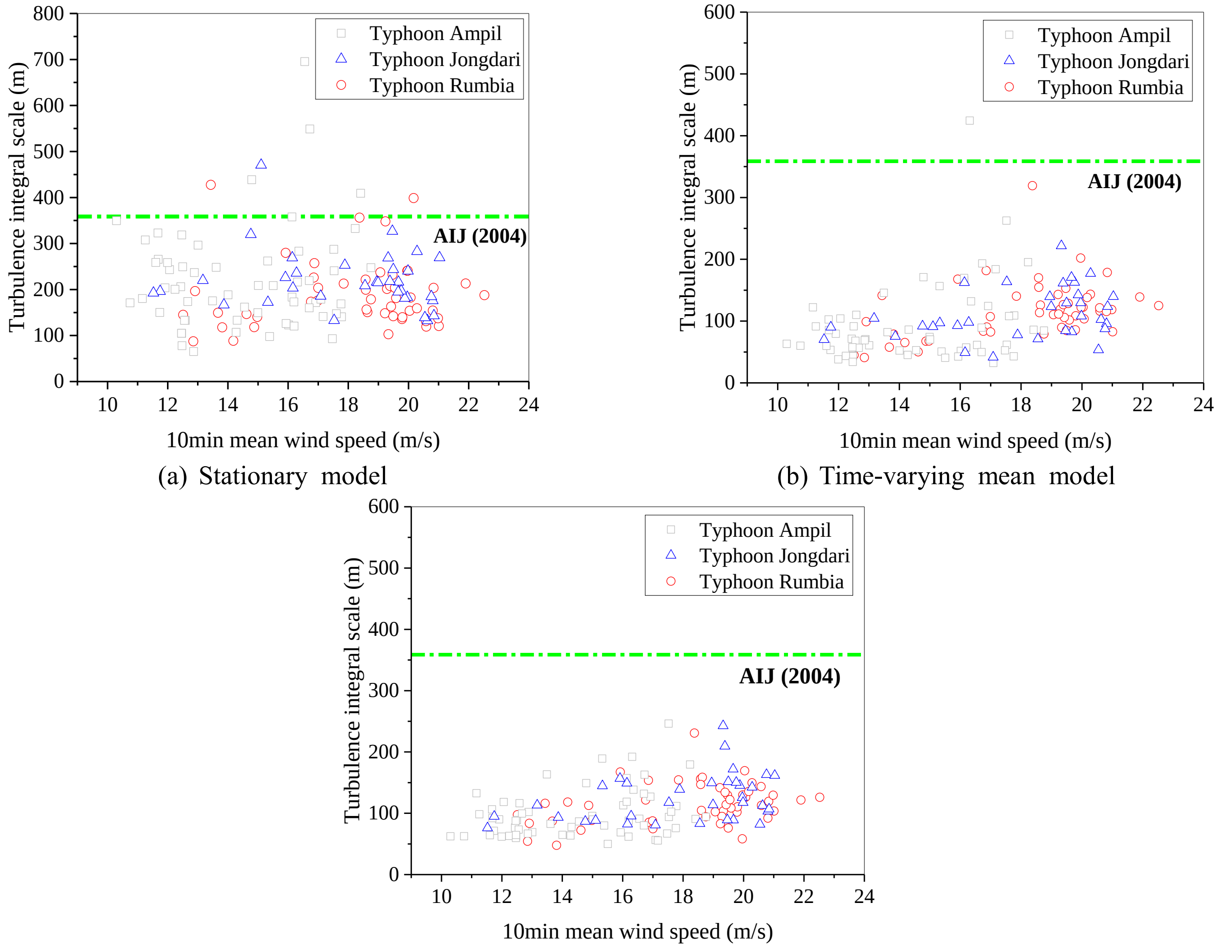


(a) Stationary model

(b) Time-varying mean model

(c) Time-varying STD model

Fig. 9. Turbulence integral scales versus the 10 min mean wind speed based on the stationary, time-varying mean, and time-varying STD wind models for the three typhoons

in the mean wind speed or fluctuating wind speed (Huang and Gu 2019a, Tao and Wang 2019). In the time-varying STD model, the measured spectra are concentrated in the large-eddy region and the inertia subregion, while the high-frequency region is slightly dispersed. Moreover, the measured spectra of the three typhoons based on the time-varying STD model have a higher similarity and approximately overlap with each other.

The Von-Karman spectra corresponding to the mean values of the turbulence integral scale of the three typhoons based on the three wind speed models are also shown in Fig. 8. As illustrated in Fig. 8, the measured spectra of the three wind speed models agree well with the Von-Karman spectra in the large-eddy region but deviate in the inertial subregion and the high-frequency region. The measured spectra of the three typhoons characterized by the time-varying STD model are the closest to the Von-Karman spectra, and the discrepancy among the different typhoons is minimal. Although there are some discrepancies between the measured spectra and Von-Karman spectra, the measured spectra are still relatively concentrated in the large-eddy region and inertia subregion, which are also the primary concerned areas in wind engineering (Tamura *et al.* 1993, Cao *et al.* 2009). Thus, as illustrated in Fig. 8, the time-varying STD model can provide more stable results of the PSDs of the longitudinal normalized fluctuating component and can better represent the common features of the different typhoons.

Fig. 9 presents the variations in the turbulence integral scale $L_u^x$ with the 10 min mean wind speed for the three wind speed models. The range, mean and standard deviation of the turbulence integral scale are also listed in Table 1.

As seen in Fig. 9 and Table 1, the dispersions of the turbulence integral scales are minimal for the time-varying STD model, moderate for the time-varying mean model, and maximal for the stationary model. The turbulence integral scales of the time-varying mean and time-varying STD models increase with the augment of mean wind speed, whereas the relationship is not notable for the stationary model. For each typhoon, the turbulence integral scales given by the stationary model are the most dispersed, and the mean value is the largest among the three wind speed models. The mean turbulent integral scales of the time-varying STD model are close to those of the time-varying mean model, but the variation range and standard deviation are smaller, indicating that the time-varying STD model can obtain more stable results.

Table 1 The statistical characteristics of the turbulence integral scales for the three typhoons

| Wind model | Typhoon type | Turbulence integral scales (m) | | |
|---|---|---|---|---|
| | | Range | Mean | Standard deviation |
| Stationary | Ampil | 65.2-695.3 | 219.3 | 111.9 |
| | Jongdari | 132.5-470.6 | 220.1 | 65.3 |
| | Rumbia | 87.3-427.6 | 189.9 | 72.7 |
| Time-varying mean | Ampil | 32.3-424.5 | 92.6 | 64.9 |
| | Jongdari | 41.5-221.9 | 112.2 | 41.3 |
| | Rumbia | 40.9-319.2 | 116.5 | 46.4 |
| Time-varying STD | Ampil | 49.8-246.3 | 98.1 | 39.9 |
| | Jongdari | 76.1-242.7 | 124.3 | 38.9 |
| | Rumbia | 47.8-230.8 | 115.1 | 33.5 |

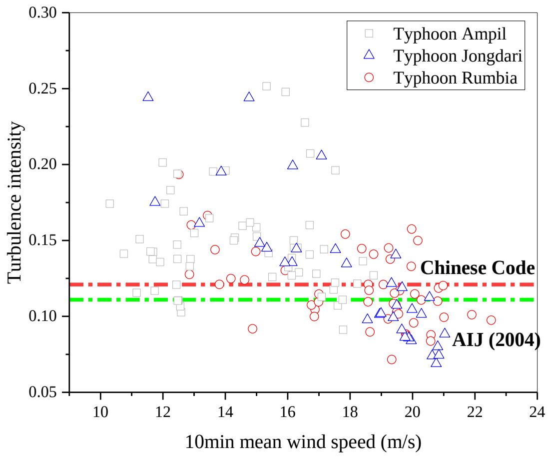


(a) Stationary model

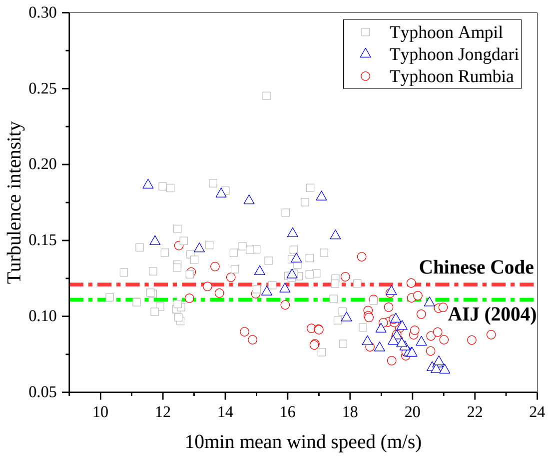


(b) Time-varying mean model

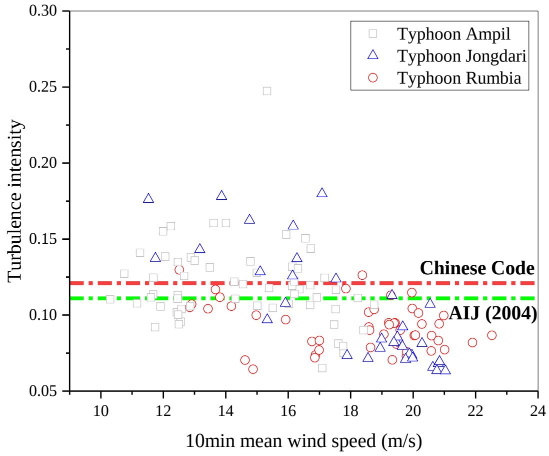


(c) Time-varying STD model

Fig. 10 Turbulence intensities based on the stationary, time-varying mean, and time-varying STD wind models for the three typhoons

For the same category and height of the observation site, the turbulence integral scale calculated based on AIJ (2004) is 358.6 m. It can be seen from Fig. 9 and Table 1 that the turbulence integral scale provided by AIJ (2004) is much larger than the mean value of the measurements for the three typhoons, which should be related to the influence of the super high-rise building cluster around the SWFC. The turbulence integral scale equation given in AIJ (2004) is mainly based on measured results over open terrains, without considering the discrepancies between different categories. The observation site in this study is located in the center of a megalopolis with an extremely rough terrain, where densely distributed high-rise and super tall buildings greatly weaken the spatial correlations of the turbulent flow, and thus the actual turbulence integral scales are dramatically decreased.

### *4.3 Turbulence Intensity*

The turbulence intensity is an important parameter to

Table 2 The statistical characteristics of the turbulence intensities for the three typhoons

| Wind model | Typhoon type | Turbulence intensities | | |
|---|---|---|---|---|
| | | Range | Mean | Standard deviation |
| Stationary | Ampil | 0.091-0.252 | 0.149 | 0.034 |
| | Jongdari | 0.069-0.244 | 0.128 | 0.047 |
| | Rumbia | 0.072-0.194 | 0.119 | 0.024 |
| Time-varying mean | Ampil | 0.077-0.245 | 0.133 | 0.029 |
| | Jongdari | 0.065-0.186 | 0.109 | 0.038 |
| | Rumbia | 0.071-0.147 | 0.100 | 0.018 |
| Time-varying STD | Ampil | 0.065-0.247 | 0.119 | 0.026 |
| | Jongdari | 0.063-0.180 | 0.103 | 0.036 |
| | Rumbia | 0.064-0.129 | 0.092 | 0.015 |

describe fluctuating wind characteristics and determine the design wind loads on structures. In the stationary model, the turbulence intensity is defined as the ratio of the standard deviation of the fluctuating wind speed to the mean wind speed for a given duration, as expressed in Eq. (9)

$$I_u = \frac{\sigma_u}{\bar{U}} \tag{9}$$

where $I_u$ is the longitudinal turbulence intensity in the stationary model; $\sigma_u$ is the standard deviation of the fluctuating wind speed; and $\bar{U}$ is the mean wind speed in a given time interval.

The turbulence intensities in the nonstationary wind speed models are defined in Eq. (10) (Huang and Gu 2019a, Wang *et al*. 2016b):

$$\begin{cases} I_u^* = E\left[\dfrac{\sigma_u^*}{U^*(t)}\right]_T \\ I_u^\Delta = E\left[\dfrac{\sigma_u^\Delta(t)}{U^\Delta(t)}\right]_T \end{cases} \tag{10}$$

where $I_u^*$ and $I_u^\Delta$ are the longitudinal turbulence intensities in the time-varying mean and time-varying STD models, respectively; $\sigma_u^*$ and $\sigma_u^\Delta(t)$ are the corresponding constant standard deviation and time-varying standard deviation, respectively, in the nonstationary wind speed models; and $E\left[\cdot\right]_T$ is the mean value over the given time interval *T*.

The relationships between the turbulence intensities and 10 min mean wind speeds of the three typhoons based on the three wind speed models are plotted in Fig. 10. The statistical characteristics of the turbulence intensities are also summarized in Table 2.

As shown in Fig. 10, the variation trends of the turbulence intensities with the mean wind speed in the three wind speed models are basically consistent. It is observed that the turbulence intensities exhibit a trend of decreasing in value and in degree of dispersion with increasing mean wind speed in the lower wind speed range, while for mean wind speed higher than 18 m/s, the turbulence intensities gradually stabilize and do not show any detectable variation trend. For each typhoon, the variation trends of the three wind speed models are similar. From Table 2, it is clear that the statistical characteristics of the turbulence intensities of the three typhoons are different. The turbulence intensities computed from the stationary model are notably larger and more scattered than those from the nonstationary wind speed models. For Typhoons Ampil, Jongdari and Rumbia, the mean values of the turbulence intensities given by the stationary model are 12.03%, 17.43% and 19.00% larger, respectively, than those of the time-varying mean model and are 25.21%, 24.27% and 29.35% larger, respectively, than those of the time-varying STD model. This phenomenon is mainly attributed to the fact that the inherent time-varying trends existing in the original wind speed records have been eliminated in the nonstationary models; thus, the stationary model may overestimate the turbulence intensities. For the two nonstationary wind speed models, the mean values and variation ranges of the time-varying STD model are smaller than those of the time-varying mean model, indicating that the time-varying STD model can give more stable results.

For the same category and height of the observation site, the recommended values of the turbulence intensities in AIJ (2004) and the Chinese code (GB5009-2012) are 0.111 and 0.121, respectively. The recommendations for the turbulence intensities are also plotted in Fig. 10 for comparison. It is worth noting that both AIJ and Chinese code recommendations are conservative in the large wind speed range. Except for Typhoon Rumbia, the mean values of the turbulence intensities calculated from the stationary model are higher than those recommended by AIJ (2004) and the Chinese code (GB5009-2012). The mean values of the turbulence intensities obtained by the nonstationary models are lower than those recommended by AIJ (2004) and the Chinese code (GB5009-2012) except for Typhoon Ampil. These discrepancies indicate the differences between the turbulence characteristics among the different typhoons and the uncertainties of the turbulence characteristics in the atmospheric boundary layer.

### *4.4 Gust factor and peak factor*

The extremum characteristics of the wind speed are also important aspects of the analysis of wind characteristics. Gust factor and peak factor are significant statistical

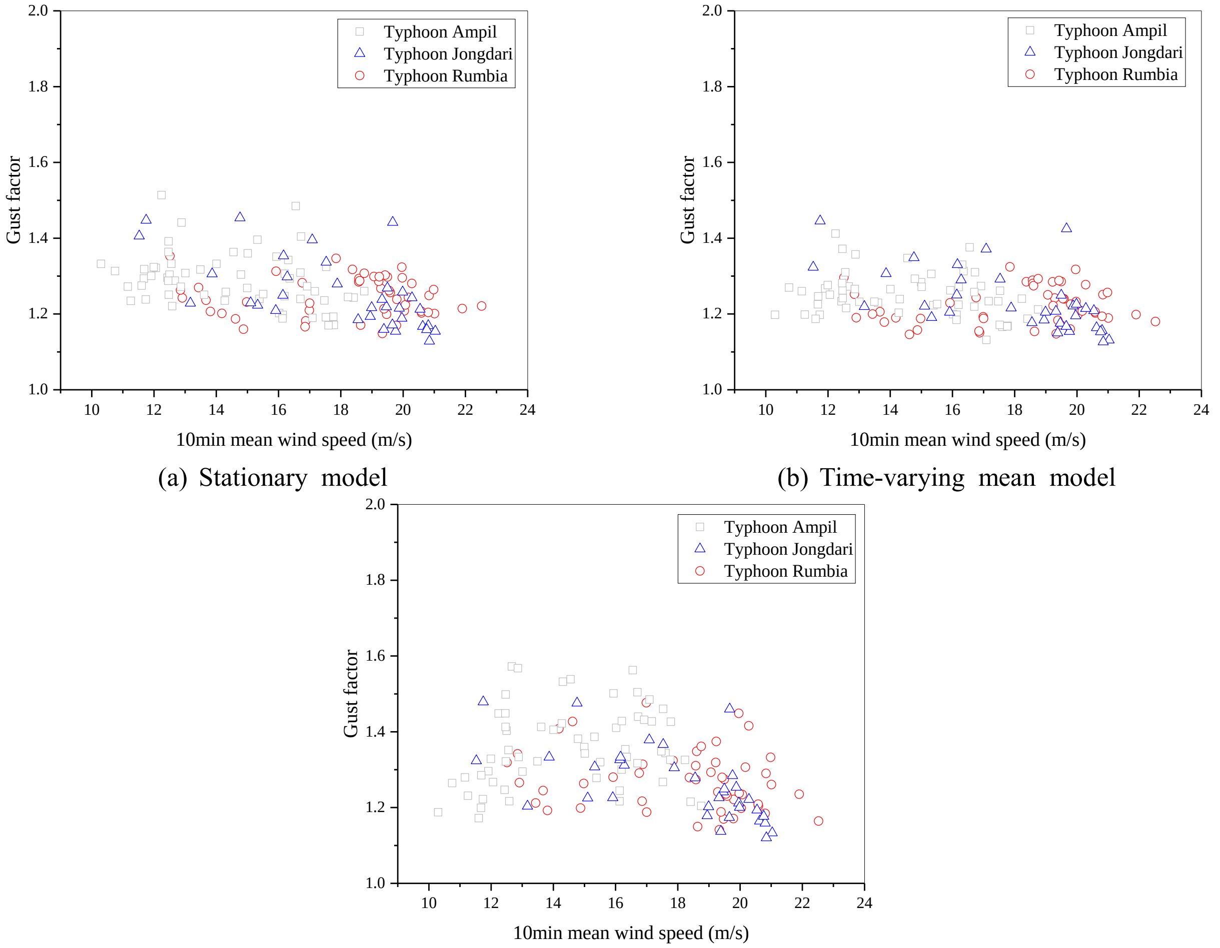


(a) Stationary model

(b) Time-varying mean model

(c) Time-varying STD model

Fig. 11 Gust factors versus the 10 min mean wind speed based on the stationary, time-varying mean, and time-varying STD wind models for the three typhoons

Table 3 The statistical characteristics of the gust factors for the three typhoons

| Wind model | Typhoon type | Gust factors | | |
|---|---|---|---|---|
| | | Range | Mean | Standard deviation |
| Stationary | Ampil | 1.17-1.51 | 1.29 | 0.07 |
| | Jongdari | 1.13-1.45 | 1.25 | 0.09 |
| | Rumbia | 1.15-1.35 | 1.25 | 0.05 |
| Time-varying mean | Ampil | 1.13-1.41 | 1.25 | 0.06 |
| | Jongdari | 1.12-1.44 | 1.23 | 0.08 |
| | Rumbia | 1.15-1.32 | 1.22 | 0.05 |
| Time-varying STD | Ampil | 1.17-1.57 | 1.35 | 0.10 |
| | Jongdari | 1.12-1.47 | 1.26 | 0.09 |
| | Rumbia | 1.14-1.47 | 1.27 | 0.08 |

parameters reflecting the ratio relationships between the maximum wind speed and the statistical characteristic values of the wind speed in a given interval, and the factors are also critical indexes for describing the intensity of the fluctuating wind speed (Shu *et al*. 2015). In the stationary model, the gust factor is the ratio of the maximum gust wind speed in a given duration to the mean wind speed over the time interval; the peak factor is the ratio of the maximum fluctuating wind speed in a given duration to the standard deviation of the fluctuating wind speed over the time interval, as defined in Eq. (11)

$$\begin{cases} G_u = \dfrac{\max\left[U(t_g)\right]_T}{\bar{U}} \\ g_u = \dfrac{\max\left[U(t_g)\right]_T - \bar{U}}{\sigma_u} \end{cases} \tag{11}$$

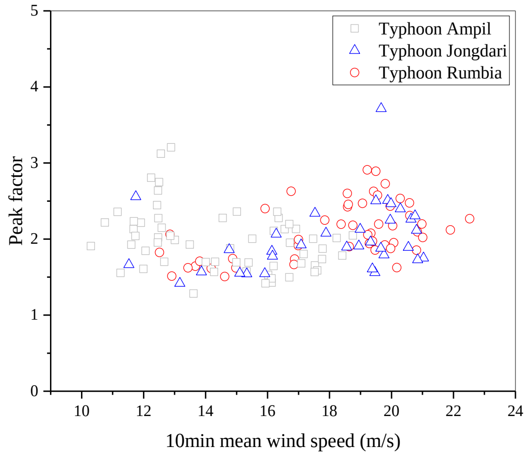

(a) Stationary model

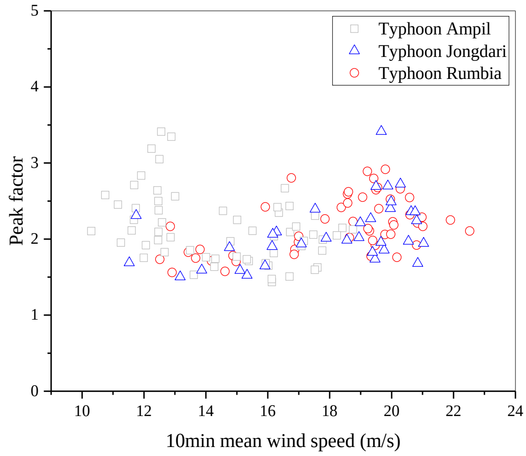

(b) Time-varying mean model

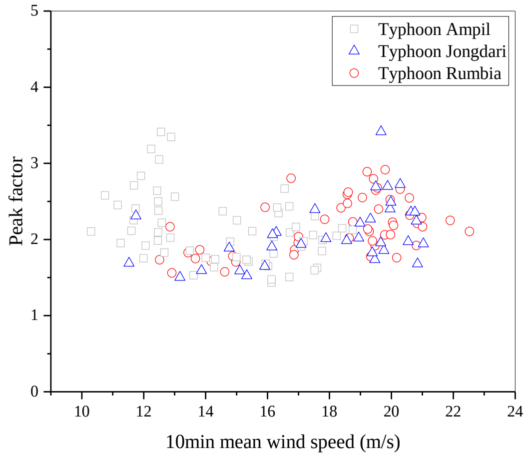

(c) Time-varying STD model

Fig. 12 Peak factors versus the 10 min mean wind speed based on the stationary, time-varying mean, and time-varying STD wind models for the three typhoons

where $G_u$ is the gust factor; $g_u$ is the peak factor; $T$ is the time interval; $\sigma_u$ is standard deviation over time interval $T$; $t_g$ is a given duration; and $U(t_g)$ is the mean wind speed over a given duration $t_g$.

In the nonstationary wind speed models, the mean wind speed and the standard deviation are not constant values but vary with time. Therefore, it is inappropriate to directly apply the forms of the stationary model formulas equations to calculate the gust factor and peak factor. A new method (Huang and Gu 2019b) for estimating the gust factor and peak factor of nonstationary wind speed models is adopted in this study. Based on the ideas of Michaelov *et al*. (2001) and Huang *et al*. (2015), the probability density function of the maximum value of the nonstationary wind speed is fitted using the probability density function of the maximum value of the equivalent Gaussian stationary wind speed, and the mean wind speed and standard deviation of the equivalent stationary wind speed are employed to normalize the maximum value of the nonstationary win speed in order to compute the gust factor and peak factor, as indicated in Eq. (12)

$$\frac{\mathrm{d}L_U(r,T)}{\mathrm{d}r}=\frac{\mathrm{d}\exp\left\{-\int_0^T v\exp\left\{-0.5\left[r-U(t)\right]^2/\sigma_U^2(t)\right\}\mathrm{d}t\right\}}{\mathrm{d}r}$$
$$\approx\frac{\mathrm{d}L_{U_{eq}}(r,T)}{\mathrm{d}r}=\frac{\mathrm{d}\exp\left\{-vT\exp\left[-0.5\left(r-\bar{U}_{eq}\right)^2/\sigma_{U_{eq}}^2\right]\right\}}{\mathrm{d}r} \tag{12}$$

where $v=\left[\int_0^{+\infty} f^2 S_\alpha(f)\mathrm{d}f\Big/\int_0^{+\infty} S_\alpha(f)\mathrm{d}f\right]^{0.5}$; $S_\alpha(f)$ is the one-sided PSD of normalized fluctuating component $\alpha_x(t)$; $L_U(r,T)$ is the cumulative distribution function of the maximum value of the nonstationary wind speed not exceeding a given value $r$; $U(t)$ is the time-varying mean wind speed; $\sigma_U(t)$ is the time-varying standard deviation; $L_{U_{eq}}(r,T)$ is the equivalent cumulative distribution function of the maximum value of the nonstationary wind speed not exceeding a given value $r$; $\bar{U}_{eq}$ is the equivalent mean wind speed; and $\bar{\sigma}_{eq}$ is the equivalent standard deviation. Hence, the

Table 4 The statistical characteristics of the peak factors for the three typhoons

| Wind model | Typhoon type | Gust factors | | |
|---|---|---|---|---|
| | | Range | Mean | Standard deviation |
| Stationary | Ampil | 1.28-3.20 | 1.98 | 0.40 |
| | Jongdari | 1.41-3.71 | 2.01 | 0.44 |
| | Rumbia | 1.51-2.91 | 2.11 | 0.37 |
| Time-varying mean | Ampil | 1.43-3.41 | 2.13 | 0.45 |
| | Jongdari | 1.50-3.42 | 2.08 | 0.41 |
| Time-varying STD | Ampil | 1.52-3.62 | 2.26 | 0.42 |
| | Jongdari | 1.44-3.76 | 2.14 | 0.44 |
| | Rumbia | 1.68-3.23 | 2.35 | 0.33 |

equivalent mean wind speed $\bar{U}_{eq}$ and the equivalent standard deviation $\bar{\sigma}_{eq}$ can be calculated with Eq. (12) via nonlinear regression, and gust factor $G_u^*$ and peak factor $g_u^*$ of the nonstationary wind speed models are computed as Eq. (13)

$$\begin{cases} G_u^* = \dfrac{\max\left[U(t_g)\right]_T}{\bar{U}_{eq}} \\ g_u^* = \dfrac{\max\left[U(t_g)\right]_T - \bar{U}_{eq}}{\bar{\sigma}_{eq}} \end{cases} \tag{13}$$

The relationships between the gust factors with 3-s gust duration and 10 min mean wind speed of the three typhoons based on the three wind speed models are shown in Fig. 11. Table 3 also summarizes the statistical characteristics of the gust factors.

As demonstrated in Fig. 11, the variation trends of the gust factors versus the mean wind speed for the three models are very similar. The gust factors decrease gradually with increasing mean wind speed. The tendencies of the gust factors with the mean wind speed for different typhoons are similar. It can be observed in Fig. 11 and Table 3 that the mean values computed by the time-varying mean model are smaller than those computed by the stationary model, and the distributions of the gust factors are also more concentrated, which is also mentioned in the works of Tao *et al*. (2016b) and Wang *et al*. (2016b). The gust factors of the time-varying STD model are slightly larger and more dispersed than those of the other two models, which is mainly because the gust factors of the time-varying STD model are not calculated directly from the time-varying mean and the time-varying standard deviation, but from the equivalent mean wind speed and the equivalent standard deviation, respectively.

## 5. Conclusions

Based on the wind speed samples of three typhoons measured atop the SWFC, the fluctuating wind characteristics obtained by the stationary model, the time-varying mean model, and the time-varying STD model are comparatively investigated in detail. The following conclusions can be drawn accordingly.

• The measured wind samples of the three typhoons show a more significant non-stationarity in the mean values than in the variances, but both types of non-stationarities cannot be neglected.

• From the results of the PDFs of the normalized fluctuation components computed by the three wind speed models, the time-varying STD model is the closest to the standard Gaussian distribution, and the distributions of the three typhoons have the least dispersion, followed by the time-varying mean model, while the stationary model performs the worst. For the PSDs, the time-varying STD model agrees well with the Von-Karman spectra for most of the components, and the spectral shapes of the three typhoons have the highest similarity, while the time-varying mean and stationary models show varying degrees of dispersion. These results indicate that the analysis results of the fluctuating wind characteristics based on the time-varying STD model are more stable and can capture the similarities of the different typhoons.

• The turbulence integral scales of the stationary model show no evident variation trend with the mean wind speed, while the turbulence integral scales of the nonstationary wind speed model increase with increasing mean wind speed. The turbulence integral scales of the time-varying STD model are the most concentrated.

• The turbulence intensities calculated by the stationary model are notably larger and more scattered than those calculated by the nonstationary wind speed models. The results of the time-varying STD model are slightly lower and more concentrated than those of the time-varying mean model.

• The gust factors first decrease gradually with increasing mean wind speed and then stabilize in the high-wind speed range. The different typhoons exhibit similar tendencies. The results of the time-varying STD model are slightly larger and more dispersed than those of the other two models.

• The peak factors generally increase slightly with increasing mean wind speed. There is not a unified regularity of the peak factor versus the mean wind speed among the three typhoons. The results of the time-varying STD model are more concentrated and, average, slightly larger than those of the other two models.

## Acknowledgments

The authors gratefully acknowledge the support from the National Natural Science Foundation of China (51778493) and the Key project of State Key Lab. of Disaster Reduction in Civil Eng. (SLDRCE19-A-05, SLDRCE19-B-13). The authors also would like to thank the Mori Building Company for providing convenient conditions during the field measurements.

## References

AIJ (2004), *Recommendations for loads on buildings*, Architectural Institute of Japan; Tokyo, Japan.

An, Y., Quan, Y. and Gu, M. (2012), "Field measurement of wind characteristics of typhoon Muifa on the Shanghai world financial center", *Int. J. Distr. Sensor Networks*. **2012**(1-3), 34-63. https://doi.org/10.1155/2012/893739.

Balderrama, J.A., Masters, F.J. and Gurley, K.R. (2012), "Peak factor estimation in hurricane surface winds", *J. Wind Eng. Ind. Aerod*., **102**(1-13). https://doi.org/10.1016/j.jweia.2011.12.003.

Bendat, J.S. and Piersol, A.G. (2011), *Random data: analysis and measurement procedures*, John Wiley & Sons, New Jersey.

Cao, S., Tamura, Y., Kikuchi, N., Saito, M., Nakayama, I. and Matsuzaki, Y. (2009), "Wind characteristics of a strong typhoon ", *J. Wind Eng. Ind. Aerod*., **97**(1), 11-21. https://doi.org/10.1016/j.jweia.2008.10.002.

Chen, J. and Xu, Y.L. (2004), "On modelling of typhoon-induced non-stationary wind speed for tall buildings", *Struct. Des. Tall Spec. Build*., **13**, 145-163. https://doi.org/10.1002/tal.247.

Chen, J., Hui, M.C.H. and Xu, Y.L. (2006), "A comparative study of stationary and non-stationary wind models using field measurements", *Bound. Lay. Meteorol*., **122**(1), 105-121. https://doi.org/10.1007/s10546-006-9085-1.

Chen, L. and Letchford, C.W. (2005), "Proper orthogonal decomposition of two vertical profiles of full-scale nonstationary downburst wind speeds[lzcl]", *J. Wind Eng. Ind. Aerod*., **93**(3), 187-216. https://doi.org/10.1016/j.jweia.2004.11.004.

Fu, J.Y., Wu, J.R., Xu, A., Li, Q.S. and Xiao, Y.Q. (2012), "Full-scale measurements of wind effects on Guangzhou West Tower", *Eng. Struct*., **35**, 120-139. https://doi.org/10.1016/j.engstruct.2011.10.022.

GB50009-2012 (2012), *The Load Code for the Design of Building Structures*, Ministry of Housing and urban-rural development of the people's Republic of China; Beijing, China.

He, X., Qin, H., Tao, T., Liu, W. and Wang, H. (2017), "Measurement of non-stationary characteristics of a landfall typhoon at the Jiangyin Bridge site", *Sensors (Basel)*, **17**(10). https://doi.org/10.3390/s17102186.

He, Y., Han, X., Li, Q. and Zhu, H. (2018), "Monitoring of wind effects on 600 m high Ping-An Finance Center during Typhoon Haima", *Eng. Struct*., **167,** 308-326. https://doi.org/10.1016/j.engstruct.2018.04.021.

Huang, C.Y., Chen, X., Liao and Li, M. (2013), "Prediction of tall building response to nonstationary winds based on multiple wind speed time history samples", *Wind Struct.* **17**(2), 227-244. https://doi.org/10.12989/was.2013.17.2.227.

Huang, G., Zheng, H., Xu, Y.L. and Li, Y. (2015), "Spectrum models for nonstationary extreme winds", *J. Struct. Eng.*, **141**(10), 04015010. https://doi.org/10.1061/(asce)st.1943-541x.0001257.

Huang, Y., Gu, M. and Huang, Z. (2019), "Field measurements of dynamic properties of a supertall building during construction of an adjacent supertall building", *J. Struct. Eng*., **145**(11), 04019121. https://doi.org/10.1061/(asce)st.1943-541x.0002391.

Huang, Z. and Gu, M. (2019a), "Characterizing nonstationary wind speed using the ARMA-GARCH Model", *J. Struct. Eng*., **145**(1), 04018226. https://doi.org/10.1061/(asce)st.1943-541x.0002211.

Huang, Z. and Gu, M. (2019b), "Estimation of peak factor and gust factor of nonstationary wind speed", *J. Wind Eng. Ind. Aerod*., **193**, 103953. https://doi.org/10.1016/j.jweia.2019.103953.

Hui, Y., Li, B., Kawai, H. and Yang, Q. (2017), "Non-stationary and non-Gaussian characteristics of wind speeds", *Wind and Structures*. **24**(1), 59-78. https://doi.org/10.12989/was.2017.24.1.059.

Law, S.S., Bu, J.Q., Zhu, X.Q. and Chan, S.L. (2006), "Wind characteristics of Typhoon Dujuan as measured at a 50 m guyed mast", *Wind Struct*., **9**(5), 387-396. https://doi.org/10.12989/was.2006.9.5.387.

Li, L., Kareem, A., Xiao, Y., Song, L. and Zhou, C. (2015), "A comparative study of field measurements of the turbulence characteristics of typhoon and hurricane winds", *J. Wind Eng. Ind. Aerod*., **140** 49-66. https://doi.org/10.1016/j.jweia.2014.12.008.

Li, Q.S. and Hu, S.Y. (2015), "Monitoring of wind effects on an instrumented low-rise building during severe tropical storm", *Wind and Struct*., **20**(3), 469-488. https://doi.org/10.12989/was.2015.20.3.469.

Li, Q.S., Wong, C.K., Fang, J.Q., Jeary, A.P. and Chow, Y.W. (2000), "Field measurements of wind and structural responses of a 70-storey tall building under typhoon conditions", *Struct. Des. Tall Build*., **9**(5), 325-342. https://doi.org/10.1002/1099-1794(200012)9:5%3C325::aid-tal169%3E3.0.co;2-b.

Li, Q.S., Xiao, Y.Q., Fu, J.Y. and Li, Z.N. (2007), "Full-scale measurements of wind effects on the Jin Mao building", *J. Wind Eng. Ind. Aerod*., **95**(6), 445-466. https://doi.org/10.1016/j.jweia.2006.09.002.

Li, Q.S., Xiao, Y.Q., Wong, C.K. and Jeary, A.P. (2003), "Field measurements of wind effects on the tallest building in Hong Kong", *Struct. Des. Tall Spec. Build*., **12**(1), 67-82. https://doi.org/10.1002/tal.213.

McCullough, M. and Kareem, A. (2013), "Testing Stationarity with Wavelet-Based Surrogates", *J. Eng. Mech*., **139**(2), 200-209. https://doi.org/10.1061/(asce)em.1943-7889.0000484.

Michaelov, G., Lutes, L.D. and Sarkani, S. (2001), "Extreme Value of Response to Nonstationary Excitation", *J. Eng. Mech*., **127**(4), 352-363. https://doi.org/10.1061/(asce)0733-9399(2001)127:4(352).

Pan, H., Xie, Z., Xu, A. and Zhang, L. (2017), "Wind effects on Shenzhen Zhuoyue Century Center: Field measurement and wind tunnel test", *Struct. Des. Tall Spec. Build*., **26**(13), e1376. https://doi.org/10.1002/tal.1376.

Quan, Y., Wang, S., Gu, M. and Kuang, J. (2013), "Field measurement of wind speeds and wind-induced responses atop the Shanghai World Financial Center under normal climate conditions", *Mathem. Probl. Eng.*, **2013** 1-14. https://doi.org/10.1155/2013/902643.

Shu, Z.R., Li, Q.S., He, Y.C. and Chan, P.W. (2015), "Gust factors for tropical cyclone, monsoon and thunderstorm winds", *J. Wind Eng. Ind. Aerod*., **142** 1-14. https://doi.org/10.1016/j.jweia.2015.02.003.

Simiu, E. and Scanlan, R.H. (1996), *Wind effects on structures: fundamentals and applications to design*, John Wiley & Sons, New York.

Song, L., Li, Q.S., Chen, W., Peng, Q., Huang, H. and He, Y.C.

(2012), "Wind characteristics of a strong typhoon in marine surface boundary layer", *Wind Struct.*, **15**(1), p.1-15. https://doi.org/10.12989/was.2012.15.1.001.

Su, Y., Huang, G. and Xu, Y.l. (2015), "Derivation of time-varying mean for non-stationary downburst winds", *J. Wind Eng. Ind. Aerod.*, **141**, 39-48. https://doi.org/10.1016/j.jweia.2015.02.008.

Tamura, Y., Shimada, K. and Hibi, K. (1993), "Wind response of a tower (Typhoon observation at the Nagasaki Huis Ten Bosch Domtoren)", *J. Wind Eng. Ind. Aerod.*, **50**, 309-318. https://doi.org/10.1016/0167-6105(93)90086-4.

Tao, T., and Wang, H. (2019), "Modelling of longitudinal evolutionary power spectral density of typhoon winds considering high-frequency subrange", *J. Wind Eng. Ind. Aerod.*, **193**, 103957. https://doi.org/10.1016/j.jweia.2019.103957.

Tao, T., Wang, H. and Li, A. (2016a), "Stationary and nonstationary analysis on the wind characteristics of a tropical storm", *Smart Struct. Systems*. **17**(6), 1067-1085. https://doi.org/10.12989/sss.2016.17.6.1067.

Tao, T., Wang, H. and Wu, T. (2016b), "Comparative study of the wind characteristics of a strong wind event based on stationary and nonstationary models", *J. Struct. Eng.*, **143**(5), 04016230. https://doi.org/10.1061/(asce)st.1943-541x.0001725.

Wang, H., Li, A., Niu, J., Zong, Z. and Li, J. (2013), "Long-term monitoring of wind characteristics at Sutong Bridge site", *J. Wind Eng. Ind. Aerod.*, **115** 39-47. https://doi.org/10.1016/j.jweia.2013.01.006.

Wang, H., Wu, T., Tao, T., Li, A. and Kareem, A. (2016), "Measurements and analysis of non-stationary wind characteristics at Sutong Bridge in Typhoon Damrey", *J. Wind Eng. Ind. Aerod.*, **151** 100-106. https://doi.org/10.1016/j.jweia.2016.02.001.

Wang, X., Huang, C., Huang, P. and Yu, X. (2017), "Study on wind characteristics of a strong typhoon in near-ground boundary layer", *Struct. Des. Tall Spec. Build.*, **26**(5), e1338. https://doi.org/10.1002/tal.1338.

Wu, J., Xu, H. and Zhang, Q. (2019), "Dynamic performance evaluation of Shanghai Tower under winds based on full-scale data", *Struct. Des. Tall Spec. Build.*, **28**(9), e1611. https://doi.org/10.1002/tal.1611.

Xiao, Y.F., Duan, Z.D., Xiao, Y.Q., Ou, J.P., Chang, L. and Li, Q.S. (2011), "Typhoon wind hazard analysis for southeast China coastal regions", *Struct. Safety*. **33**(4-5), 286-295. https://doi.org/10.1016/j.strusafe.2011.04.003.

Xu, Y.L. and Chen, J. (2004), "Characterizing nonstationary wind speed using empirical mode decomposition", *J. Struct. Eng.*, **130**(6), 912-920. https://doi.org/10.1061/(asce)0733-9445(2004)130:6(912).

Xu, Y.L., Zhu, L.D., Wong, K.Y. and Chan, K.W.Y. (2000), "Field measurement results of Tsing Ma suspension Bridge during Typhoon Victor", *Struct. Eng. Mech.*, **10**(6). https://doi.org/10.12989/sem.2000.10.6.545.

Xu, Z., Wang, H., Wu, T., Tao, T. and Mao, J. (2017), "Wind characteristics at sutong bridge site using 8-year field measurement data", *Wind Struct.*, **25**(2), 195-214. https://doi.org/10.12989/was.2017.25.2.195.

Yu, C., Li, Y., Zhang, M., Zhang, Y. and Zhai, G. (2019), "Wind characteristics along a bridge catwalk in a deep-cutting gorge from field measurements", *J. Wind Eng. Ind. Aerod.*, **186** 94-104. https://doi.org/10.1016/j.jweia.2018.12.022.

Zhi, L., Li, Q.S., Wu, J.R. and Li, Z.N. (2011), "Field monitoring of wind effects on a super-tall building during typhoons", *Wind Struct.*, **14**(3), p.253-283. https://doi.org/10.12989/was.2011.14.3.253.

*FR*